

Article

## Coal Char Derived Few-Layer Graphene Anodes for Lithium Ion Batteries

Dan Wang, Santosh H. Vijapur and Gerardine G. Botte \*

Center for Electrochemical Engineering Research, Chemical and Biomolecular Engineering Department, Ohio University, Athens, OH 45701, USA; E-Mails: wangd@ohio.edu (D.W.); sv239405@ohio.edu (S.H.V.)

\* Author to whom correspondence should be addressed; E-Mail: botte@ohio.edu; Tel.: +1-740-593-9670; Fax: +1-740-593-0873.

Received: 18 July 2014; in revised form: 18 August 2014 / Accepted: 18 August 2014 /

Published: 25 August 2014

---

**Abstract:** Few-layer graphene films were synthesized through chemical vapor deposition technique using coal char as solid carbon source. Raman spectroscopy, X-ray diffraction, transmission electron microscopy, and selected area electron diffraction were used to characterize the graphene films. The electrochemical performance of the coal char derived few layer graphene anodes for lithium ion batteries was investigated by charge/discharge curves and discharge capacity at different current densities. The graphene anode maintained the reversible capacity at  $\sim 0.025$ ,  $0.013$ , and  $0.007$  mAh/cm<sup>2</sup> at a current density of 10, 30, and 50  $\mu$ A/cm<sup>2</sup>, respectively. The coal char derived graphene anodes show potential applications in thin film batteries for nanoelectronics.

**Keywords:** graphene; coal char; coal electrolysis; chemical vapor deposition; lithium ion batteries

---

### 1. Introduction

Graphene has been gaining much attention in the past decade due to its excellent physical/chemical properties and its uses in various potential applications ranging from electronics to composites and sensors [1–6]. Graphene has been synthesized through different methods, such as micromechanical cleavage technique, liquid exfoliation method, epitaxial growth, total organic synthesis, and chemical vapor deposition (CVD) [1,6,7]. Among all the methods, CVD is the most promising method for

growing high quality and large area graphene films. Inspired by its superb electrical and optical properties, large specific surface area, and excellent chemical stability, the CVD grown graphene shows great potential in the applications of sensing [8,9], energy storage and generation [10,11], and corrosion science [12,13].

The traditional CVD methods require hydrocarbon gas as a carbon source, which limit the applications of this technology to various potential carbon feedstocks. Recently, solid carbon sources, such as poly(methyl methacrylate), sucrose, polystyrene, and amorphous carbon thin film have drawn interest for use as carbon sources in pristine graphene film growth using the CVD method [14–16]. Coal and food waste have further exhibited promise as low cost carbon feedstocks for graphene synthesis [17,18].

Coal is a carbon-enriched abundant natural source. Other than the well-known coal gasification and liquefaction for producing syngas and synthetic fuels, coal electrolysis has been recently demonstrated as a powerful technique for hydrogen production in a clean and efficient manner. [19–23] The electrolyzed coal (coal char) is the by-product or the waste of this process. However, it is also the potential inexpensive solid carbon source for graphene film production. [24–26] Within this context, the objective of this work is to synthesize graphene films using the coal char, which is the waste of coal electrolysis, as a solid carbon source through CVD process. This work also investigated the electrochemical performance of the coal char derived few layer graphene films used as anodes for lithium ion batteries. The graphene films are grown on copper substrates, and thus directly used as anodes for lithium ion batteries without any aid of polymer binders and conductive fillers. The graphene anodes have potential applications in thin film batteries, which are the power sources for micro/nano devices, such as implantable medical micromachines and on-chip memory [27,28].

## 2. Experimental Section

### 2.1. Chemicals and Materials

Copper foils (99.8%, 0.025 mm thickness) were obtained from Alfa Aesar. Acetone (>99%), cupric sulfate (>95%), hydrochloric acid (6N), sulfuric acid (18 N), and reagent grade ferric sulfate were purchased from Fisher Scientific. Iron (II) sulfate heptahydrate (>99%) was purchased from Acros Organics. Lithium hexafluorophosphate ( $\text{LiPF}_6$ , 12.4wt%) in ethylene carbonate (EC, 43.8wt%) and diethyl carbonate (DEC, 43.8wt%) was purchased from BASF.

Pittsburgh #8 coal was used for coal electrolysis and graphene synthesis. This coal is classified as a high volatile A bituminous coal and was obtained from the Penn State coal bank. The elemental analysis of the Pittsburgh #8 coal (provided by the coal bank) reported carbon (74.69%), hydrogen (4.98%), nitrogen (1.23%), organic sulfur (0.73%), oxygen (6.49%), and mineral matter (11.88%) content. The coal obtained was subjected to grinding, sieving and shuffling to achieve a uniform coal particle size of <210  $\mu\text{m}$ .

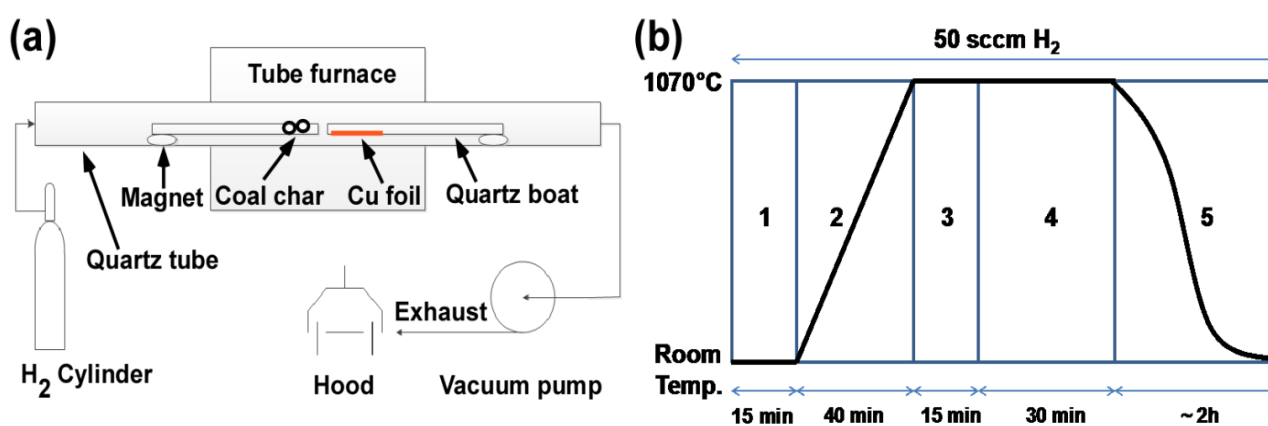
### 2.2. Graphene Synthesis

Coal char was obtained as the by-product of coal electrolysis and used as a solid carbon source for graphene growth. The detailed description and schematic of coal electrolysis have been discussed in

previous work [19,23]. Only a brief description is given here: The continuous coal electrolytic cell (CEC) designed and constructed by Jin and Botte was used for the coal electrolysis. [19] The anolyte and catholyte reservoirs were filled with 300 mL of 4 M  $\text{H}_2\text{SO}_4$ , which was used as an electrolyte. Iron (II) sulfate heptahydrate and iron (III) sulfate were used as sources for iron ions (40 mM  $\text{Fe}^{2+}$ /40 mM  $\text{Fe}^{3+}$ ) and added to the anodic solution. Coal was added to the anodic solution to obtain a coal slurry concentration of 0.04 g/mL. The solution in the anolyte (coal and iron ions in sulfuric acid) and catholyte (sulfuric acid) reservoirs was stirred at 300 rpm throughout the electrolysis processing time. The operating current density used was  $100 \text{ mA/cm}^2$  and the temperature was set to  $104 \text{ }^\circ\text{C}$ . An Arbin battery cycler (BT-2000) was used to conduct the coal electrolysis using a galvanostatic method. A cut-off voltage was set to 1.17 V to avoid the electrolysis of water and the oxidation of the electrode support. Typical electrolysis processing time was  $\sim 8.5 \text{ h}$ .

After coal electrolysis, the coal char was collected and dried at  $70 \text{ }^\circ\text{C}$  in an oven over night. The dried electrolyzed coal char was used then for the synthesis of graphene through CVD. Figure 1a shows the schematic of the CVD system for graphene synthesis. 10 mg of dried coal char and a piece of copper foil ( $1.5 \text{ cm} \times 6.0 \text{ cm}$ ) were placed on the end of two quartz boats separately. Magnets were attached on other end of the two quartz boats for moving the quartz boats during the synthesis. There are five steps in a typical graphene synthesis experiment as shown in Figure 1b. First, the CVD system was evacuated and backfilled with hydrogen (99.999% purity) at a flow rate of 50 sccm for 15 min. Second, the tube furnace was heated to  $1070 \text{ }^\circ\text{C}$  in 40 min. Third, the quartz boat with copper foil was moved into the tube furnace for 15 min of annealing. Fourth, the quartz boat with coal char was shifted into the heating zone for graphene synthesis on the copper foil. After 30 min of graphene growth, the quartz boats were moved out of the furnace and cooled down to room temperature.

**Figure 1.** (a) Schematic of chemical vapor deposition (CVD) system for graphene synthesis using electrolyzed coal char. (b) Synthesis procedure showing operating conditions: time, temperature, and gas flow rate for the growth of graphene films.



### 2.3. Graphene Characterization

In order to characterize the synthesized graphene films, the copper foil substrates were first dissolved in a solution mixture of 10 g  $\text{CuSO}_4$ , 50 mL  $\text{HCl}$ , and 50 mL DI water. The graphene films were then observed to be floating in the solution. The floating graphene film was next transferred to DI

water using a clean glass slide to clean the surface of the graphene film and remove any contamination. Finally, the graphene films were lifted onto the silicon wafers, XRD sample holder, and transmission electron microscopy (TEM) copper grids for Raman, XRD, and TEM characterization, respectively. The Raman spectra were collected on a Bruker Senterra Raman spectrometer through a 20 X objective lens using an argon laser ( $\lambda = 532$  nm) with 20 mW power. XRD patterns of graphene film and coal char were obtained on a Rigaku Ultima IV X-Ray Diffractometer with monochromatic Cu  $K\alpha$  radiation ( $\lambda = 0.15405$  nm) at a scanning rate of  $0.2^\circ \text{min}^{-1}$ . TEM images and the selected area electron diffraction (SAED) of the graphene films were acquired using the JEM 2100 F transmission electron microscope (JEOL).

#### 2.4. Electrochemical Analysis

Electrochemical measurements were carried out in a split test cell (MTI Corporation) using a Solartron 1470 potentiostat. The test cells were assembled in an argon-filled glovebox ( $\text{O}_2 < 1$  ppm and  $\text{H}_2\text{O} < 1$  ppm, Mbraun). The CVD-grown graphene on copper foils were punched to discs, which have 1.27 cm in diameter, and directly used as anodes. Lithium foils and Celgard 2500 microporous monolayer membranes were used as counter/reference electrodes and separators, respectively.  $\text{LiPF}_6$  (12.4wt%) in EC (43.8wt%) and DEC (43.8wt%) was used as the electrolyte (BASF, LP40). Galvanic charge-discharge cycles were performed between 0.01 V and 3.00 V.

### 3. Results and Discussion

#### 3.1. Characterizations of Graphene Films

The Raman spectrum of CVD-grown graphene films (Figure 2a; red curve) shows three major peaks: the D band at  $\sim 1347$   $\text{cm}^{-1}$ ; G band at  $\sim 1573$   $\text{cm}^{-1}$ ; and 2D band at  $\sim 2682$   $\text{cm}^{-1}$ . The D band is attributed to defects in the graphene films and G band is due to the tangential vibrations of  $\text{sp}^2$  bonded carbon atoms. The presence of the 2D band indicates the graphene feature of the synthesized films; which results from the two phonon double resonances in second order Raman spectra associated with graphene. [29,30] In the control experiments; the coal char only show the broad D band at  $\sim 1346$   $\text{cm}^{-1}$  and G band at  $\sim 1594$   $\text{cm}^{-1}$  (Figure 2a; black curve); indicating the amorphous features of coal char. [31] The XRD patterns of the graphene film and coal char are shown in Figure 2b. The diffraction peak at  $\sim 26^\circ$  corresponds to (002) reflection of graphene (Figure 2b; red curve). As a comparison, the black curve (Figure 2b) indicates coal char contains minerals such as kaolinite (K), magnetite (M), quartz (Q), illite (I) and siderite (S), which agrees well with reported results of electrolyzed Pittsburgh No. 8 coal [32].

**Figure 2.** Raman spectra (a) and XRD patterns (b) of coal char derived graphene (red curve) and coal char (black curve).

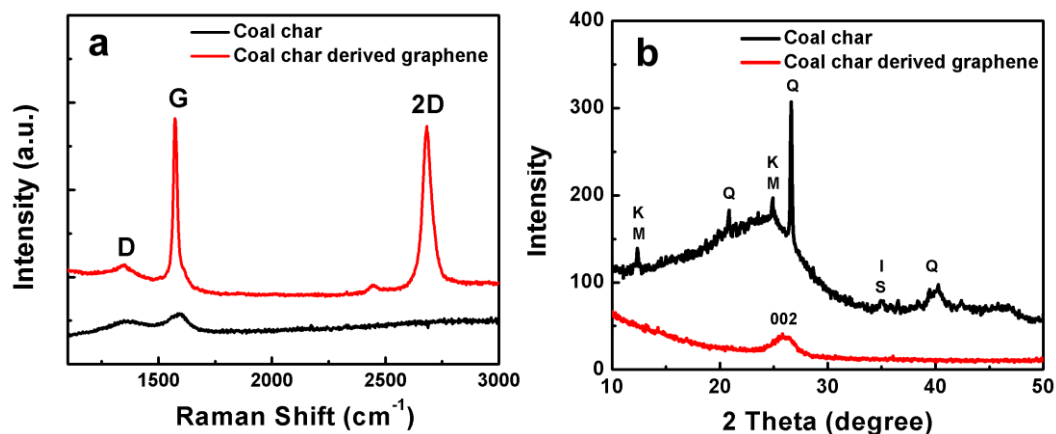
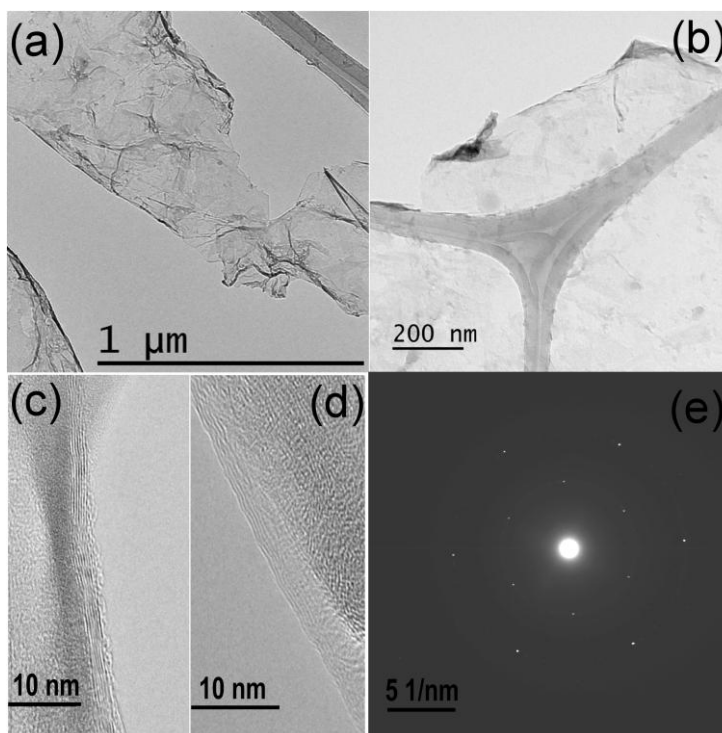


**Figure 3.** TEM images of large area and continuous graphene films (a,b). High-resolution TEM images of the edges of synthesized graphene films (c,d). Hexagonal selected area electron diffraction (SAED) pattern of the graphene films (e).



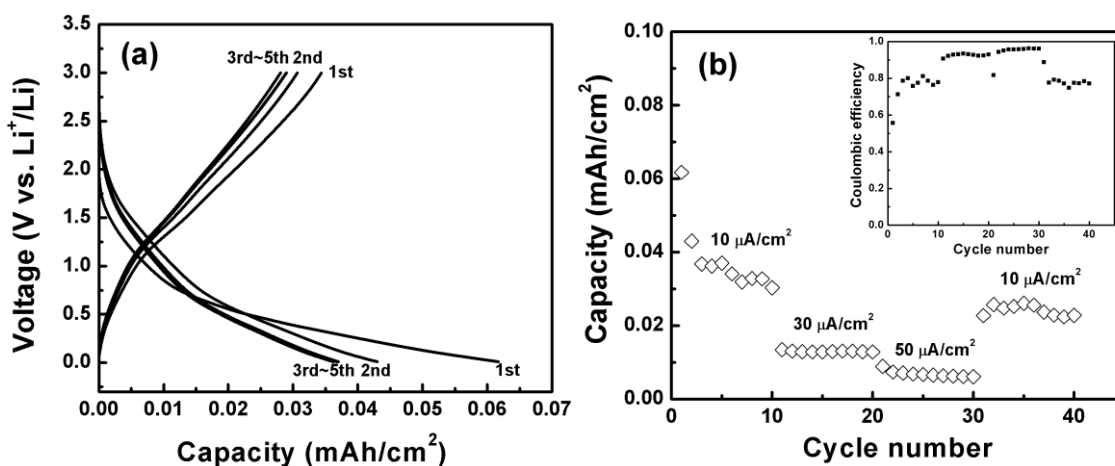
The morphology and structure of graphene films were further characterized by TEM as shown in Figure 3. Figure 3a and 3b show continuous graphene films over a large area with the formation of wrinkles, back-folding and overlapping of edge due to the transfer process. Figure 3c and 3d were randomly imaged edges of graphene films under TEM. The results indicate most of the graphene films have 4–7 layers. The typical hexagonal crystalline structure of graphene was examined by SAED pattern (Figure 3e). The six diffraction spots in the SAED pattern confirm the single crystalline nature of graphene films [29,33].

De Abreu *et al.* provided characterizations of Pittsburgh No. 8 coal after electrolysis. [32] Aromatic type films are present on the surface of the coal after electrolysis. It is hypothesized that the films on the surface of the coal enable the synthesis of graphene. It is worth mentioning that Pittsburgh No. 8 coal without electrolysis did not enable the synthesis of graphene films at the conditions used in the CVD process. The electrolyzed coal in the CVD synthesis goes through a similar process as coal pyrolysis. Coal pyrolysis at high temperature (>400 °C) in an anaerobic atmosphere will release hydrocarbons. [34,35] The released hydrocarbons are the precursors for graphene growth and are adsorbed on the surface of copper substrates to form active carbon species during the CVD process [17,36]. After nucleation and growth of the adsorbed active carbon species, the graphene films are synthesized on the copper foil surfaces [14,15].

### 3.2. Electrochemical Analysis of Graphene Anodes

Figure 4a shows the charge-discharge curves of the first five cycles of coal char derived graphene anode at a current density of 10  $\mu\text{A}/\text{cm}^2$  between 3.00 V and 0.01 V vs Li/Li<sup>+</sup>. The first discharge capacity is ~0.062 mAh/cm<sup>2</sup> and reduced to ~0.043 mAh/cm<sup>2</sup> in the second cycle. The loss in capacity is due to the formation of solid electrolyte interface (SEI) layer on the graphene surface. [11,27,30] The reversible capacity is maintained at ~0.030 mAh/cm<sup>2</sup> in the following cycles at a current density of 10  $\mu\text{A}/\text{cm}^2$ , which is comparable with the reported capacity of tens of layer-graphene anodes. [11] Figure 4b shows cycling curves of discharge capacity at different current densities (10, 30, and 50  $\mu\text{A}/\text{cm}^2$ ). The graphene anode exhibits reversible capacity of ~0.013 mAh/cm<sup>2</sup> at current density of 30  $\mu\text{A}/\text{cm}^2$  and ~0.007 mAh/cm<sup>2</sup> at current density of 50  $\mu\text{A}/\text{cm}^2$ . When the current density returns to 10  $\mu\text{A}/\text{cm}^2$ , the reversible capacity is maintained at ~0.025 mAh/cm<sup>2</sup>. The inset of Figure 4b shows the corresponding coulombic efficiencies at different cycle numbers of the graphene anode.

**Figure 4.** Charge-discharge curves of coal char derived graphene anode at 10  $\mu\text{A}/\text{cm}^2$  between 3.00 V and 0.01 V vs Li/Li<sup>+</sup> (a). Discharge capacity vs. cycle numbers at different current densities (10, 30, and 50  $\mu\text{A}/\text{cm}^2$ ), (b). Inset: the corresponding coulombic efficiencies vs. cycle numbers.



#### 4. Conclusions

Electrolyzed coal (coal char) was used as solid carbon sources for synthesizing few-layer graphene films through the CVD method. Raman spectrum of the synthesized films shows 2D band feature of graphene. The TEM images and SAED pattern show morphology and typical hexagonal crystalline structure of graphene films, respectively. The electrolyzed coal char derived few layer graphene films were tested as anodes for lithium ion batteries and showed the reversible capacity at  $\sim 0.025$  mAh/cm<sup>2</sup> at a current density of 10  $\mu$ A/cm<sup>2</sup> after 40 charge-discharge cycles at different current densities (10, 30, and 50  $\mu$ A/cm<sup>2</sup>).

#### Acknowledgments

The authors would like to thank the financial support from the Center for Electrochemical Engineering Research (CEER) at Ohio University, the Ohio Department of Development Office of Energy (Ohio Coal Demonstration and Pilot Program) Grant # OOE-CDO-D-13-23, and the National Science Foundation through the Major Research Instrumentation Grant # CBET-1126350.

#### Author Contributions

Gerardine G. Botte developed the idea for the technology, provided working hypothesis, participated in the analysis of results, and mentored researchers. Dan Wang and Santosh H. Vijapur designed the experimental matrix and synthesized the graphene. Santosh H. Vijapur carried out the coal electrolysis experiments. Dan Wang fulfilled the characterization of graphene and the electrochemical analysis of graphene anodes. All authors contributed in the writing of this paper.

#### Conflict of Interest

The authors declare no conflict of interest.

#### References

1. Allen, M.J.; Tung, V.C.; Kaner, R.B. Honeycomb Carbon: A Review of Graphene. *Chem. Rev.* **2010**, *110*, 132–145.
2. Geim, A.K. Graphene: Status and Prospects. *Science* **2009**, *324*, 1530–1534.
3. Geim, A.K.; Novoselov, K.S. The rise of graphene. *Nat. Mater.* **2007**, *6*, 183–191.
4. Pumera, M. Graphene-based nanomaterials for energy storage. *Energy Environ. Sci.* **2011**, *4*, 668–674.
5. Rao, C.N.R.; Biswas, K.; Subrahmanyam, K.S.; Govindaraj, A. Graphene, the new nanocarbon. *J. Mater. Chem.* **2009**, *19*, 2457–2469.
6. Rao, C.N.R.; Sood, A.K.; Subrahmanyam, K.S.; Govindaraj, A. Graphene: The New Two-Dimensional Nanomaterial. *Angew. Chem. Int. Ed.* **2009**, *48*, 7752–7777.
7. Bonaccorso, F.; Lombardo, A.; Hasan, T.; Sun, Z.; Colombo, L.; Ferrari, A.C. Production and processing of graphene and 2D crystals. *Mater. Today* **2012**, *15*, 564–589.

8. Kwak, Y.H.; Choi, D.S.; Kim, Y.N.; Kim, H.; Yoon, D.H.; Ahn, S.-S.; Yang, J.-W.; Yang, W.S.; Seo, S. Flexible glucose sensor using CVD-grown graphene-based field effect transistor. *Biosens. Bioelectron.* **2012**, *37*, 82–87.
9. Chen, T.-Y.; Loan, P.T.K.; Hsu, C.-L.; Lee, Y.-H.; Tse-Wei Wang, J.; Wei, K.-H.; Lin, C.-T.; Li, L.-J. Label-free detection of DNA hybridization using transistors based on CVD grown graphene. *Biosens. Bioelectron.* **2013**, *41*, 103–109.
10. Kim, H.; Bae, S.-H.; Han, T.-H.; Lim, K.-G.; Ahn, J.-H.; Lee, T.-W. Organic solar cells using CVD-grown graphene electrodes. *Nanotechnology* **2014**, doi:10.1088/0957-4484/25/1/014012.
11. Radhakrishnan, G.; Cardema, J.D.; Adams, P.M.; Kim, H.I.; Foran, B. Fabrication and Electrochemical Characterization of Single and Multi-Layer Graphene Anodes for Lithium-Ion Batteries. *J. Electrochem. Soc.* **2012**, *159*, A752–A761.
12. Prasai, D.; Tuberquia, J.C.; Harl, R.R.; Jennings, G.K.; Rogers, B.R.; Bolotin, K.I. Graphene: Corrosion-Inhibiting Coating. *ACS Nano* **2012**, *6*, 1102–1108.
13. Singh Raman, R.K.; Chakraborty Banerjee, P.; Lobo, D.E.; Gullapalli, H.; Sumandasa, M.; Kumar, A.; Choudhary, L.; Tkacz, R.; Ajayan, P.M.; Majumder, M. Protecting copper from electrochemical degradation by graphene coating. *Carbon* **2012**, *50*, 4040–4045.
14. Ji, H.; Hao, Y.; Ren, Y.; Charlton, M.; Lee, W.H.; Wu, Q.; Li, H.; Zhu, Y.; Wu, Y.; Piner, R.; Ruoff, R.S. Graphene Growth Using a Solid Carbon Feedstock and Hydrogen. *ACS Nano* **2011**, *5*, 7656–7661.
15. Li, Z.; Wu, P.; Wang, C.; Fan, X.; Zhang, W.; Zhai, X.; Zeng, C.; Li, Z.; Yang, J.; Hou, J. Low-Temperature Growth of Graphene by Chemical Vapor Deposition Using Solid and Liquid Carbon Sources. *ACS Nano* **2011**, *5*, 3385–3390.
16. Sun, Z.; Yan, Z.; Yao, J.; Beitler, E.; Zhu, Y.; Tour, J.M. Growth of graphene from solid carbon sources. *Nature* **2010**, *468*, 549–552.
17. Vijapur, S.H.; Wang, D.; Botte, G.G. Raw coal derived large area and transparent graphene films. *ECS Solid State Lett.* **2013**, *2*, M45–M47.
18. Ruan, G.; Sun, Z.; Peng, Z.; Tour, J.M. Growth of Graphene from Food, Insects, and Waste. *ACS Nano* **2011**, *5*, 7601–7607.
19. Jin, X.; Botte, G.G. Feasibility of hydrogen production from coal electrolysis at intermediate temperatures. *J. Power Sources* **2007**, *171*, 826–834.
20. Hesenov, A.; Meryemoglu, B.; Icten, O. Electrolysis of coal slurries to produce hydrogen gas: Effects of different factors on hydrogen yield. *Int. J. Hydrogen Energy* **2011**, *36*, 12249–12258.
21. Hesenov, A.; Kinik, H.; Puli, G.; Gozmen, B.; Irmak, S.; Erbatur, O. Electrolysis of coal slurries to produce hydrogen gas: Relationship between CO<sub>2</sub> and H<sub>2</sub> formation. *Int. J. Hydrogen Energy* **2011**, *36*, 5361–5368.
22. Yu, T.; Lv, S.; Zhou, W.; Cao, W.; Fan, C.Q.; Yin, R. Catalytic effect of K<sub>3</sub>Fe(CN)<sub>6</sub> on hydrogen production from coal electro-oxidation. *Electrochim. Acta* **2012**, *83*, 485–489.
23. Jin, X.; Botte, G.G. Understanding the kinetics of coal electrolysis at intermediate temperatures. *J. Power Sources* **2010**, *195*, 4935–4942.
24. Botte, G.G. Pretreatment method for the synthesis of carbon nanotubes and carbon nanostructures from coal and carbon chars (Div. 2); U.S. Patent No. 8409305 B2, 2013.

25. Botte, G.G. Pretreatment method for the synthesis of carbon nanotubes and carbon nanostructures from coal and carbon chars (Div. 1); U.S. Patent No. 8409305, 2013.
26. Botte, G.G. Pretreatment method for the synthesis of carbon nanotubes and carbon nanostructures from coal and carbon chars; U.S. Patent No. 8029759, 2011.
27. Reddy, A.L.M.; Srivastava, A.; Gowda, S.R.; Gullapalli, H.; Dubey, M.; Ajayan, P.M. Synthesis Of Nitrogen-Doped Graphene Films For Lithium Battery Application. *ACS Nano* **2010**, *4*, 6337–6342.
28. Li, C.-L.; Sun, Q.; Jiang, G.-Y.; Fu, Z.-W.; Wang, B.-M. Electrochemistry and Morphology Evolution of Carbon Micro-net Films for Rechargeable Lithium Ion Batteries. *J. Phys. Chem. C* **2008**, *112*, 13782–13788.
29. Robertson, A.W.; Warner, J.H. Hexagonal Single Crystal Domains of Few-Layer Graphene on Copper Foils. *Nano Lett.* **2011**, *11*, 1182–1189.
30. Wei, D.; Haque, S.; Andrew, P.; Kivioja, J.; Ryhaenen, T.; Pesquera, A.; Centeno, A.; Alonso, B.; Chuvilin, A.; Zurutuza, A. Ultrathin rechargeable all-solid-state batteries based on monolayer graphene. *J. Mater. Chem. A* **2013**, *1*, 3177–3181.
31. Potgieter-Vermaak, S.; Maledi, N.; Wagner, N.; Van Heerden, J.H.P.; Van Grieken, R.; Potgieter, J.H. Raman spectroscopy for the analysis of coal: a review. *J. Raman Spectrosc.* **2011**, *42*, 123–129.
32. De Abreu, Y.; Patil, P.; Marquez, A.I.; Botte, G.G. Characterization of electrooxidized Pittsburgh No. 8 Coal. *Fuel* **2006**, *86*, 573–584.
33. Geng, D.; Wu, B.; Guo, Y.; Huang, L.; Xue, Y.; Chen, J.; Yu, G.; Jiang, L.; Hu, W.; Liu, Y. Uniform hexagonal graphene flakes and films grown on liquid copper surface. *P. Natl. Acad. Sci. USA* **2012**, *109*, 7992–7996.
34. Fuchs, W.; Sandhoff, A.G. Theory of Coal Pyrolysis. *Ind. Eng. Chem.* **1942**, *34*, 567–571.
35. Miknis, F.P.; Turner, T.F.; Ennen, L.W.; Netzel, D.A. N.m.r. characterization of coal pyrolysis products. *Fuel* **1988**, *67*, 1568–1577.
36. Vijapur, S.H.; Wang, D.; Botte, G.G. The growth of transparent amorphous carbon thin films from coal. *Carbon* **2013**, *54*, 22–28.

© 2014 by the authors; licensee MDPI, Basel, Switzerland. This article is an open access article distributed under the terms and conditions of the Creative Commons Attribution license (<http://creativecommons.org/licenses/by/3.0/>).